

Extrinsic Calibration Between a 3D Laser Scanner and a Camera Under Interval Uncertainty

Raphael Voges*and Bernardo Wagner

Leibniz Universität Hannover, Real Time Systems Group (RTS)
Appelstraße 9A, D-30167 Hannover, Germany
{voges,wagner}@rts.uni-hannover.de

Keywords: Extrinsic calibration; Camera; 3D LiDAR; Interval analysis; Contractors

Introduction

For navigation in the absence of GPS, mobile robots often fuse information from both laser scanner and camera to take advantage of both sensor modalities [1]. While the laser scanner allows to measure accurate distances to the environment, camera images can be employed to re-identify salient features over time and space. However, to fuse data from both sensors, the extrinsic transformation - i.e. the rotation and translation between the sensor coordinate systems - has to be known.

Generally, all approaches for the extrinsic calibration between camera and laser scanner can be divided into two categories: target-based (e.g. using a checkerboard) or target-less (by relying on natural image features). Since the target-less extrinsic calibration is usually less accurate due to the problem of accurately identifying the same features in both laser scan and camera data, we omit it and focus on the target-based calibration. Unnikrishnan and Hebert employ a checkerboard for which they extract the plane parameters from the data of both sensors [2]. Since their approach requires corresponding plane parameters from at least three different checkerboard poses, Zhou et al. aim to reduce this number by incorporating additional features into their non-linear optimization [3]. Instead of only extracting the checkerboard's plane, they

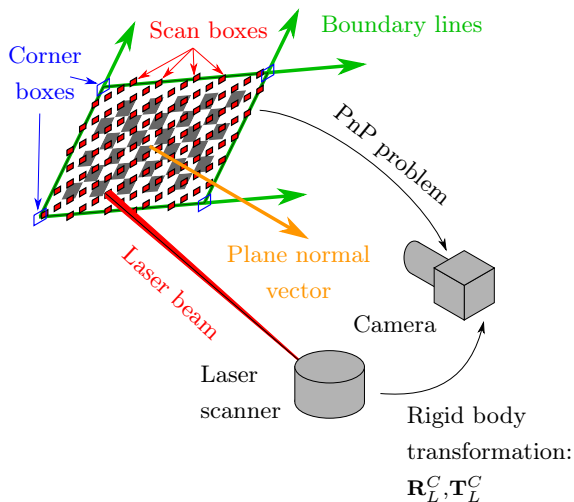


Figure 1: To find the rigid body transformation between camera and laser scanner, consisting of the rotation \mathbf{R}_L^C and the translation \mathbf{T}_L^C , we extract plane, line and point features from the data of both sensors.

also identify the border lines in both the camera image and the laser scan. Consequently, the authors integrate these line features as additional constraints, and can thus reduce the number of required checkerboard poses while also increasing the calibration accuracy.

However, both presented approaches neglect the underlying uncertainties and their accuracies can only be assessed by comparing the resulting transformation to ground truth information. This poses a problem since ground truth is generally not available and the results from Zhou et al. show that the accuracy varies significantly with the number and diversity of chosen checkerboard poses [3].

Furthermore, both approaches assume zero-

*Corresponding author.

mean noise for the sensors. However, prior to the extrinsic laser-camera calibration, an intrinsic camera calibration needs to be performed. Here, imperfections leading to biased intrinsic camera parameters can occur. Subsequently, these parameters are employed to establish a connection between image pixels and real world coordinates, resulting in biased (non-zero-mean) features for the following extrinsic calibration. Likewise, the laser scanner’s distance and angular measurements can be biased due to an imperfect calibration, leading to systematic errors for the extracted plane and line features.

Thus, we propose to assign an unknown but bounded error to the sensor measurements and use interval analysis to propagate the error from input sources to the final calibration result. On the one hand, this allows us to model unknown systematic errors for both sensors. On the other hand, we can immediately assess the extrinsic calibration accuracies by inspecting the corresponding interval widths. Similar work - although for a different application - has been done by Sandretto et al., who introduce a method to calibrate a cable-driven robot [4].

Extrinsic Calibration

We extract the same plane and line features as proposed by Zhou et al. [3], but constrain the rigid body transformation even further by computing the checkerboard’s corner points. Figure 1 shows the general idea. All computations are performed in a bounded-error context, meaning that we start by modeling the sensor errors with intervals and extract interval domains for the desired features.

To identify the aforementioned features in the camera image, we solve the Perspective-n-Point problem under interval uncertainty [5]. This allows us to establish a connection between the camera coordinate system and the checkerboard coordinate system. By taking advantage of the fact that the dimensions of

the checkerboard are known, we can immediately compute a box enclosing the corner points and derive the boundary lines as well as the plane parameters accordingly.

To find the plane parameters in the laser scan data, we force the corresponding interval boxes on a common plane by employing a forward-backward contractor in combination with branching. Subsequently, we find boundary points residing on the checkerboard’s border and fit a line through them to determine the boundary lines. Afterwards, a box enclosing the corner points can be computed by intersecting adjacent boundary lines.

In the following, we introduce the variables required to establish the constraint satisfaction problem (CSP). Generally, a right superscript C or L indicates that the particular feature is given in the camera or laser scanner coordinate system, respectively.

- \mathbf{n}^L and \mathbf{n}^C are the unit checkerboard plane normal vectors.
- \mathbf{d}_i^L and \mathbf{d}_i^C are unit direction vectors describing the same checkerboard boundary line $i \in \{1, \dots, 4\}$.
- \mathbf{Q}_{ij}^L and \mathbf{Q}_{ik}^C are points on the line i with $j \in \{1, \dots, N_i\}$ and $k \in \{1, 2\}$. N_i is the total number of points on the line i which we extract from laser scan data. In contrast, we determine only two points on every line i for the camera - namely the two adjacent corner points.
- \mathbf{P}_l^L are scan points on the checkerboard with $l \in \{1, \dots, N_p\}$. N_p is the total number of scan points on the plane.
- d^C is the distance from the camera coordinate system’s origin to the plane.
- \mathbf{C}_m^L and \mathbf{C}_m^C are corresponding checkerboard corner points, $m \in \{1, \dots, 4\}$.

Finally, we are able to formulate the CSP that employs the extracted features to constrain the rigid body transformation, which consists of the rotation matrix \mathbf{R}_L^C and the translation vector \mathbf{T}_L^C .

x	ϕ_L^C (°)	θ_L^C (°)	ψ_L^C (°)	xT_L^C (cm)	yT_L^C (cm)	zT_L^C (cm)
x^*	90.0	0.0	0.0	-27.0	15.0	-12.0
$[x]$	[89.6, 90.3]	[-0.4, 0.3]	[-0.1, 0.3]	[-28.8, -25.0]	[13.1, 16.7]	[-13.1, -11.0]
$w([x])$	0.7	0.7	0.4	3.8	3.6	2.1

Table 1: Results from simulation. The rotation matrix \mathbf{R}_L^C is expressed using the three Euler angles θ_L^C , ψ_L^C and ϕ_L^C . Besides, $\mathbf{T}_L^C = (xT_L^C \ yT_L^C \ zT_L^C)^\top$. We depict the true transformation parameters x^* , the computed intervals $[x]$ and the corresponding interval widths $w([x])$.

Variables: $\mathbf{R}_L^C, \mathbf{T}_L^C, \mathbf{n}^L, \mathbf{n}^C, \mathbf{d}_i^L, \mathbf{d}_i^C,$
 $\mathbf{Q}_{ij}^L, \mathbf{Q}_{ik}^C, \mathbf{P}_l^L, d^C, \mathbf{C}_m^L, \mathbf{C}_m^C$

Constraints:

1. $\mathbf{R}_L^C \mathbf{n}^L = \mathbf{n}^C$
2. $\mathbf{R}_L^C \mathbf{d}_i^L = \mathbf{d}_i^C$
3. $(\mathbf{I} - \mathbf{d}_i^C (\mathbf{d}_i^C)^\top) (\mathbf{R}_L^C \mathbf{Q}_{ij}^L + \mathbf{T}_L^C - \mathbf{Q}_{ik}^C) = 0$
4. $\mathbf{n}^C \cdot (\mathbf{R}_L^C \mathbf{P}_l^L + \mathbf{T}_L^C) + d^C = 0$
5. $\mathbf{R}_L^C \mathbf{C}_m^L + \mathbf{T}_L^C = \mathbf{C}_m^C$

Domains: $[\mathbf{R}_L^C], [\mathbf{T}_L^C], [\mathbf{n}^L], [\mathbf{n}^C], [\mathbf{d}_i^L], [\mathbf{d}_i^C],$
 $[\mathbf{Q}_{ij}^L], [\mathbf{Q}_{ik}^C], [\mathbf{P}_l^L], [d^C], [\mathbf{C}_m^L], [\mathbf{C}_m^C]$

To solve the CSP, we build a forward-backward contractor for all constraints. In principle, one corresponding laser scan and camera image suffices to compute the transformation. However, by combining the contractors built from different checkerboard poses, the accuracy can be increased.

Results

Our results for simulated data show that we are able to reliably enclose the true transformation parameters for different transformations. The results indicate that our method can cope with outliers by employing a q-relaxed intersection and performs accurately for different error intervals. Table 1 depicts exemplary results.

Moreover, we collected data using a typical laser scanner and camera setup to demonstrate the applicability of our approach to real data. The resulting intervals are consistent

with the parameters computed using the approach of Zhou et al. [3]. Unlike their method, however, our approach allows a direct assessment of the accuracy.

Acknowledgement

This work was supported by the German Research Foundation (DFG) as part of the Research Training Group i.c.sens [RTG 2159].

References

- [1] R. Voges, C. S. Wiegardt, and B. Wagner, “Finding timestamp offsets for a multi-sensor system using sensor observations”, *Photogrammetric Engineering & Remote Sensing*, vol. 84, no. 6, pp. 357–366, 2018.
- [2] R. Unnikrishnan and M. Hebert, “Fast Extrinsic Calibration of a Laser Rangefinder to a Camera”, 2005.
- [3] L. Zhou, Z. Li, and M. Kaess, “Automatic Extrinsic Calibration of a Camera and a 3D LiDAR Using Line and Plane Correspondences”, in *2018 IEEE/RSJ International Conference on Intelligent Robots and Systems (IROS)*, Oct. 2018.
- [4] J. A. D. Sandretto, G. Trombettoni, D. Daney, and G. Chabert, “Certified Calibration of a Cable-Driven Robot Using Interval Contractor Programming”, in *Computational Kinematics*, Springer Netherlands, Oct. 2013, pp. 209–217.
- [5] R. Voges and B. Wagner, “Timestamp Offset Calibration for an IMU-Camera System Under Interval Uncertainty”, in *IEEE/RSJ International Conference on Intelligent Robots and Systems (IROS)*, Oct. 2018.